# A Multivariate Variational Objective Analysis - Assimilation Method, Part I: Development of the Basic Model

Gary L. Achtemeier and Harry T. Ochs III
Climate and Meteorology Section
Illinois State Water Survey
Champaign, Illinois 61820, USA

# A Multivariate Variational Objective Analysis - Assimilation Method, Part I: Development of the Basic Model

Gary L. Achtemeier and Harry T. Ochs III
Climate and Meteorology Section
Illinois State Water Survey
Champaign, Illinois 61820, USA

## ABSTRACT

The variational method of undetermined multipliers is used to derive a multivariate model for objective analysis. The model is intended for the assimilation of three-dimensional fields of rawinsonde height, temperature and wind and mean level temperature observed by satellite into a dynamically consistent data set. Relative measurement errors are taken into account. The dynamic equations are the two nonlinear horizontal momentum equations, the hydrostatic equation, and an integrated continuity equation. The model Euler-Lagrange equations are eleven linear and/or nonlinear partial differential and/or algebraic equations. A cyclical solution sequence is described.

Other model features include a nonlinear terrain-following vertical coordinate that eliminates truncation error in the pressure gradient terms of the horizontal momentum equations and easily accommodates satellite observed mean layer temperatures in the middle and upper troposphere. A projection of

the pressure gradient onto equivalent pressure surfaces removes most of the adverse impacts of the lower coordinate surface on the variational adjustment.

An evaluation of the variational objective analysis model appears in the following companion paper.

## 1. Introduction

The accurate diagnosis the state of the atmosphere with data measured from space-based platforms requires that these data be merged with data collected routinely by traditional methods. Because of diversities in variables measured, measurement accuracy, observation location, and observation density, it becomes necessary to do the blending in a way that the final analyses is at least an approximate solution of some mathematical relationship between the variables.

The creation of a multivariate data set that is consistent with the mathematical expressions for the behavior of air in the free atmosphere is more typically accomplished through some form of data assimilation coupled with an initialization for a numerical prediction model. Observational data is blended with model forecast fields through an interpolation technique (Cressman, 1959; Gandin, 1963; Schlatter; 1975) in which the latter, used as a first guess, is updated with the observations. These methods are multivariate; wind observations are used in the interpolative analysis of the height and temperature fields and vice versa. Then an initialization procedure such as dynamic initialization (e.g., Miyakoda and Moyer, 1968; Nitta and Hovermale,

1969) or normal mode initialization (e.g., Baer and Tribbia, 1977; Machenhaur, 1977; Daley, 1981) brings the hybrid data set into consistency with a numerical model equation set. Highly sophisticated dynamically consistent data assimilation schemes such as those described by McPherson, et al., (1979), Bengtsson, et al., (1982), Ghil, et al., (1979), Temperton (1984), and many others produce accurate representations of the state of the synoptic scale atmosphere. These hybrid data sets, though modified to be consistent with the scales of motion permitted by the models, also may be useful for diagnostic studies.

This paper describes a nonlinear multivariate objective analysis for which the constrained state is defined by primitive equations. The purpose of this study is to achieve the dynamically constrained merger of satellite data with traditional data and to assess the impact of the former upon the analysis. The method is diagnostic. It does, however, require estimates for the explicitly formulated local tendencies of the velocity components and temperature which might be provided by a numerical model. The completed diagnostic scheme will contain complex mathematical constraints that are similar to those found in sophisticated methods for data assimilation and initialization of numerical models. This study focuses on the diagnostics of cyclone systems, including precipitation systems within cyclone systems, whereas many studies of numerical forecasts with mixed data sets are focused upon improved forecast skill. However, the completed model may eventually be of value in comparisons with existing data assimilations. The basic model (MODEL I) derived through methods of variational calculus is described herein and a companion paper (Achtemeier, et al., 1988) deals with an evaluation of the method using a case study.

The goal of our research is the development of a variational data assimilation method that incorporates as dynamical constraints, the primitive equations for a moist, convectively unstable atmosphere and the radiative transfer equation. Variables that can be included in the adjusted are the three-dimensional vector wind, height, temperature, and moisture from rawinsonde data, and cloud-wind vectors, moisture, and radiance from satellite data. This presents a formidable mathematical problem. In order to facilitate thorough analysis of each of the model components, we defined four variational models that divide the problem naturally according to increasing complexity. The first variational model (MODEL I) contains the two nonlinear horizontal momentum equations, the integrated continuity equation, and the hydrostatic equation. Problems associated with an internally consistent finite difference method, a nonlinear hybrid terrain-following vertical coordinate, formulations for the pressure gradient terms, formulations for the velocity tendency terms and the development of a convergent solution sequence are addressed with MODEL I and are the subject of this paper.

MODEL II contains MODEL I plus the thermodynamic equation for a dry adiabatic atmosphere. The introduction of this additional constraint violates the requirement that the number of subsidiary conditions (dynamic constraints) must be at least one less than the number of dependent variables (Courant, 1936). Inclusion of the same number of constraints as dependent variables overdetermines the problem and a solution is not guaranteed. Therefore, we will design MODEL I to increase the number of dependent variables. MODEL III contains MODEL II plus an additional moisture variable and an equation to describe moist adiabatic processes. MODEL IV includes MODEL III plus radiance

as a dependent variable and the radiative transfer equation as a constraint.

The next section presents the philosophy of a variational objective analysis model. In Section 3 appear the dynamic equations in the forms they enter the variational formalism as constraints. The variational equations are derived in Section 4. Details concerning the grid mesh, boundary conditions, and convergence of the equations are found in Section 5. Section 6 summarizes the model.

## 2. A Variational Approach to Diagnostic Data Assimilation

Our diagnostic objective analysis is an adaptation of Sasaki's (1958) method of variational analysis. Data from different measurement systems are weighted according to measurement accuracies and are blended using a least squares method into a hybrid data set that satisfies a set of subsidiary conditions. Sasaki (1970a) presented two variational formulations for the solution of the data assimilation problem. His "weak constraint" formalism requires only a partial satisfaction of the subsidiary conditions through coefficients determined by the analyst. The subsidiary conditions are satisfied exactly through the "strong constraint" method. Ikawa (1984) has shown that the weak constraint algorithm converges to the strong constraint formalism as the coefficients become large.

This study makes use of the method of undetermined multipliers (strong constraint formalism). The constraints are the nonlinear horizontal momentum equations (products of a variational principle (Wang, 1984)), the hydrostatic

equation and an integrated form of the continuity equation. The adjustments are carried out on fields of meteorological variables obtained through univariate objective interpolation. This kind of variational formulation has been criticized by Williamson and Daley (1983) on the grounds that the adjustments to the dynamic state are carried out from gridded fields rather than from the observations. Alternatively, observation statistics for different measurements of the same variable can be carried in the analyzed fields, perhaps as proposed by Baker (1983). Another approach would blend the variational analysis with a optimized successive corrections methods similar to that proposed by Bratseth (1986).

Another difficulty with the method of undetermined multipliers is the complexity of the variational equations which stimulates a need for simpler methods to create hybrid, dynamically balanced data sets. Wahba and Wendelberger (1980) have shown that multivariate statistical objective analysis and variational analysis are interchangeable for linear constraints. Our variational method permits nonlinear constraints, allows for the physical interpretation of the adjustments and provides mutual adjustment between the mass and wind fields (Temperton, 1984).

Accurately gridded meteorological variables are a requirement for any good diagnostic analysis. There are also quantities which, because of poor instrument accuracy or insufficient sampling frequency, cannot be measured directly and must be inferred through functions of other measured variables; in our case, they are products of the variational blending process. Among these are hypersensitive variables such as vertical velocity and the local tendencies of the horizontal velocity components, that are sensitive to small

changes in the other variables. The variational diagnostic model must also produce accurate fields of these hypersensitive variables.

Krishnamurti (1968) calculated diagnostic vertical velocities through a 12-forcing function balance omega equation. More recently, Smith and Lin (1978) preferred vertical velocities diagnosed from the O'Brien (1970) variational method. Our variational model calculates vertical velocity from a generalized form of the kinematic method for which the O'Brien method can be shown to be a special case.

The local tendency terms of the horizontal velocity components are particularly difficult to determine accurately because the coarse sampling frequency of operational data collection networks is not sufficient to resolve the frequency of meteorological disturbances. Local tendencies can be incorporated into the variational analysis by fixing them and assuming that the generated error will not appreciably contaminate the solution. But this ignores the fact that the tendency terms are of the same order of magnitude as the advection terms and that generated error undoubtedly will contaminate the solution, especially the error sensitive divergence calculations. Sasaki (1970b), Sasaki and Lewis (1970), and Lewis and Grayson (1972) have used a "time-wise localized" method which physically is not a time adjustment, but a space filter designed to adjust variables in space at a particular time such that the local tendency is minimized with partial constraint satisfaction. Achtemeier (1975) included local rates of change in a primitive equation variational model through a subsidiary variational formulation based upon O'Brien's (1970) divergence adjustment method. This method was considered a failure after an extensive analysis (Achtemeier, 1979) found unrealistically

large velocity component tendencies where actual velocity changes over a 12-hr period were small.

More recently, Lewis (1980, 1982) has examined the problem of time consistency from a Lagrangian approach through the application of Thompson's (1969) variational method. Lewis et al., (1983) and Lewis and Derber (1985) combined rawinsonde data with VAS height data taken 2.5 hr later and found vertical velocity fields that compared favorably with space-observed cloud fields and surface weather reports. These studies and the results from Bloom's (1983) mesoscale analysis imply that variational methods can be used with some success in the direct determination of tendency variables, at least for observation frequencies on the order of 3-hr.

## 3. The Formulations for the Dynamic Constraints

The dynamic constraints, $M_i$, for MODEL I are the two nonlinear horizontal momentum equations, the hydrostatic equation, and an integrated continuity equation. These constraints must undergo several transformations for the successful solution of the variational problem with the method of undetermined Lagrange multipliers. The equations are nondimensionalized following the methodology of Charney (1948) and Haltiner (1971). These equations transform into a nonlinear terrain-following vertical coordinate. Another transformation removes a hydrostatic component introduced into lower coordinate surfaces by unlevel terrain and thermodynamic variables are partitioned to give reference and perturbation atmospheres. The reference atmosphere is dynamically consistent. The variational analyses are done on the perturbation variables.

Following Shuman and Hovermale (1968), the horizontal momentum equation,

for the u-component (eastward directed component at a reference longitude) of the three-dimensional vector wind, nondimensionalized in an arbitrary vertical coordinate and Cartesian on a conformal projection of the earth is,

$$R_o \left[\frac{\partial u}{\partial x} + m\left(u\frac{\partial u}{\partial x} + v\frac{\partial u}{\partial y}\right) + \dot{\sigma}\frac{\partial u}{\partial \sigma}\right] - v(f+\gamma) + m\left(\frac{\partial \phi}{\partial p}\frac{\partial p}{\partial x} + \frac{\partial \phi}{\partial x}\right) + F_x = 0 \qquad (1)$$

where conventional meteorological symbols are used. Anthes and Warner (1978) show that $\gamma$, a distortion that arises from the projection of points on a sphere on to a conformal surface, is at least two orders of magnitude smaller than f and can be neglected. The projection ratio, m, is defined for a Lambert conformal projection. As part of the nondimensionalization, the mapscale factor, m, and the Coriolis parameter, f, expand into $m=1+R_1K$ and $f=1+R_1C$ where the arrays K and C are of order one and $R_1=0.1$.

The nondimensionalized hydrostatic equation in the generalized vertical coordinate is,

$$\frac{\partial \phi}{\partial \sigma} + T\frac{\partial \ln p}{\partial \sigma} = 0 \qquad (2)$$

a) Vertical Coordinate for the Variational Assimilation Model

The vertical coordinate follows the concept of Phillips (1957). It blends from a terrain-following coordinate in the lower troposphere into a pressure coordinate in the middle troposphere. All horizontal variations with the lower coordinate surface are confined to levels below a reference pressure level $p^*$. This vertical coordinate has the following advantages for the variational assimilation model:

(1) The dynamical equations are presented in their simplest form on the pressure surfaces at and above $p^*$. Coding to omit terms that are zero for coordinate surfaces that are surfaces of constant pressure can result in a substantial reduction of computational overhead. The tradeoff is that the equations below $p^*$ are more complex than the equations written for the linear sigma coordinate. However, the magnitudes of these additional terms become small in the sigma levels above the lower coordinate surface.

(2) All coordinate surfaces at and above p* are pressure surfaces. Vertical interpolation of initial fields of data, such as mean layer temperatures from satellite observations that function with pressure, is not required for these coordinate surfaces. Furthermore, there is no need to interpolate from sigma coordinates back to pressure coordinates in order to interpret the variationally adjusted fields of meteorological variables.

(3) Where coordinate surfaces are not constant pressure surfaces, the pressure gradient terms of the horizontal momentum equations transform into two large and compensating terms where there is steep, sloping terrain. The variational formalism will separate the pressure gradient terms and combine the large uncompensated terms with terms from the other equations. The large nonmeteorological impacts by these terms can cause significant error in the final solution. The nonlinear vertical coordinate eliminates this problem for the middle and upper troposphere (coordinate surfaces above the elevation of $p^*$.) A partition to reduce the impacts by these terms for layers below $p^*$ is the subject of section b). The smooth transition from the terrain-following to the pressure coordinate is accomplished by fitting two curves which are piecewise continuous through the second derivatives. The curve for the upper

layer bounded by $p_u$ at the top and by $p^*$ at the bottom is given by a straight line subject to the boundary conditions that $\sigma=0$ at $p=p_u$ and that $\sigma=\sigma^*$ at $p=p^*$. This equation is

$$\sigma = \sigma^* \frac{p-p_u}{p^*-p_u} \tag{3}$$

The equation for the nonlinear part of the hybrid vertical coordinate between $p^*$ and the surface pressure $p_s$ is found subject to the following four conditions:

$$\left.\begin{aligned} \sigma &= 1.0 && \text{at } p=p_s \\ \sigma &= \sigma^* \\ \frac{\partial\sigma}{\partial p} &= \sigma^*/(p^*-p_u) \\ \frac{\partial^2\sigma}{\partial p^2} &= 0\ . \end{aligned}\right\} \quad \text{at } p=p^* \tag{4}$$

These four conditions specify the equation as a cubic polynomial which takes the form

$$\sigma = \beta\,(p-p^*)^3 + \sigma^* \frac{(p-p_u)}{(p^*-p_u)} \tag{5}$$

$$\beta = \left[1- \sigma^* \left(\frac{p_s-p_u}{p^*-p_u}\right)\right] (p_s-p^*)^{-3} \tag{6}$$

Fig. 1 shows the relationship between sigma and pressure for the levels below the elevation of the 600 mb pressure surface for the coordinate parameters that have been selected for the variational assimilation. The reference pressure $p^*$ is at 700 mb. A straight line from 700 mb to 1000 mb separates two sets of curves which describe the relationship between sigma and pressure for low surface pressure (high elevation) from those for high surface pressure. Wherever the slopes of the curves in Fig. 1 are less than the slope

of the straight line, the pressure thicknesses between sigma coordinate surfaces are compacted. The smallest pressure thicknesses are found nearest the lower coordinate surface. These layer depths increase to approach the thicknesses of the pressure layers at levels above $p^*$.

The slopes of the curves in Fig. 1 exceed the slope of the straight line at locations where the surface pressure is greater than 1000 mb. The pressure thicknesses between the sigma coordinate surfaces have been expanded. Note how the curve from 1100 mb converges asymptotically into the straight line by p=900mb. The nonlinear vertical coordinate forces most of the transition between terrain-following coordinate surfaces and pressure-following coordinate surfaces into the layer immediately above the ground. Thus coordinate surfaces in the lower troposphere tend to behave as pressure surfaces that are punctuated by areas of higher elevation.

Fig. 2 shows the distribution of coordinate surfaces below 600 mb as the surface pressure varies from 800 to 1025 mb, the approximate range of surface pressures for the smoothed orography of the variational model. The greater compression of the coordinate surfaces over higher elevation nearest the surface is clearly evident. Notice how the nonlinear coordinate surfaces tend to become surfaces of constant pressure at locations away from the areas of high elevation. Note also the increased pressure depth of the lowest layer where the surface pressures exceed 1000 mb. Clearly this nonlinear vertical coordinate does not provide for a boundary layer of uniform thickness.

b) Partition to Reduce Impact of Nonmeteorological Hydrostatic Terms

Below $p^*$ where coordinate surfaces are not constant pressure surfaces, the pressure gradient terms of the horizontal momentum equations transform into two large and compensating terms where there is steep, sloping terrain. The variational formalism separates these pressure gradient terms and combines the large uncompensated terms with terms from the other equations. The impacts by these terms can introduce significant error into the final solution. This problem can be avoided by partitioning the hydrostatic equation into terrain terms and meteorological perturbation terms and subjecting the latter to the variational operation. Note that what is done is a partitioning, not a transformation. There is no change in the vertical coordinate.

Consider the geopotential height and temperature in (2) to contain the "whole" signal and partition them into terrain, reference, initial, and adjusted variables according to,

$$( )_w = ( )_T + ( )_R + ( )^0 + [( ) - ( )^0] \qquad (7)$$

Furthermore, partition the whole pressure into

$$p_w = p_T + p_e \qquad (8)$$

where the subscript, e, identifies "equivalent" pressure surfaces as a distinction between the adjustable heights obtained by this method and the heights of the pressure surfaces from the original observations. Upon partitioning, the hydrostatic equation can be expressed as the sum of four

groups of terms. These are:

Terrain,

$$\left[\left(\frac{p_w}{p_e} - 1\right) \frac{\partial \phi_w^o}{\partial \sigma} + \frac{\partial \phi_T}{\partial \sigma} + \frac{T_w^o}{p_e} \frac{d \ln p_T}{\partial \sigma}\right] \tag{9}$$

Reference,

$$\left[\frac{\partial \phi_R}{\partial \sigma} + \gamma T_R\right] \tag{10}$$

Adjustment,

$$\left[\left(\frac{p_w}{p_e} - 1\right) \frac{\partial}{\partial \sigma} (\phi - \phi^o) + \frac{(T-T^o)}{p_e} \frac{\partial \ln p_T}{\partial \sigma}\right] \tag{11}$$

Perturbation,

$$\left[\frac{\partial \phi}{\partial \sigma} + \gamma T\right] \tag{12}$$

where $\gamma = \partial \ln(p_e)/\partial \sigma$ . Since the subscript w terms are known from the observations, the terrain height and its vertical gradient may be found from the specification of $p_e$ and requiring the terrain group to sum to zero. An accurate solution depends upon specification of a representative pressure for each layer. After some experimentation, it was found that, if the equivalent pressure at the top and the bottom of the layer is known, the average of the arithmetic mean plus twice the geometric mean,

$$p = \frac{1}{3} \left[\frac{1}{2} (p_2 + p_1) + 2 \sqrt{p_2 p_1}\right] \tag{13}$$

gives an accurate representative pressure.

Fig. 3a shows the heights of the lower coordinate surface at 1200 GMT 10 April 1979 without partitioning of the hydrostatic equation. The figure shows

mostly the variation of elevation. Fig. 3b shows the meteorological heights analyzed to the 1000 mb pressure surface. The low, about 100 mb deep over Colorado, is an order of magnitude smaller than the height of the smoothed terrain. Fig. 3c shows the heights of the 1000 mb equivalent pressure surface after partitioning the hydrostatic equation. The resemblance of all features to the heights of the actual 1000 mb surface is evident except for the higher central height of the low center over Colorado. The underestimation of this feature occurred because colder temperatures at higher elevations (the terrain temperature) were not partitioned. Since we have merely partitioned the heights, not neglected height terms, the remaining heights that make up the difference in the heights between Fig. 3c and Fig. 3b are spread among the remaining three groups of terms that make up the hydrostatic equation.

Upon removal of the terrain height, the heights are averaged over each level to obtain the reference height. Then a hydrostatic reference atmosphere is found by requiring the reference group of terms to sum to zero.

The residual group includes the small part of the terrain group that is subject to variation. These terms tend to compensate. Since the variational adjustments are only few tenths to one degree Kelvin, the residual terms are at least two orders of magnitude smaller than the comparable terrain terms and are one order of magnitude smaller than the perturbation terms. If the adjustment terms are represented by $\beta$, then the hydrostatic equation is given by,

$$\frac{\partial \phi}{\partial \sigma} + \gamma T + \beta = 0 \qquad (14)$$

Once the hydrostatic equation is partitioned, the pressure gradient terms of the horizontal momentum equations can be partitioned to reduce the impacts of unlevel terrain. The partitioned pressure gradient term from (1) is,

$$PGX = \frac{\partial \phi}{\partial x} + \eta_x \qquad (15)$$

where,

$$\eta_x = (T-T^o) \frac{\partial \ln p_T}{\partial x} + \eta_x^o \qquad (16)$$

is the sum of a small term subject to variation and unadjusted compensatory terrain terms,

$$\eta_x^o = \frac{\partial \phi_T}{\partial x} + T_w^o \frac{\partial \ln p_T}{\partial x} \qquad (17)$$

c) Partition of the Local Tendencies

Local changes in the horizontal velocity components are caused by a combination of translation of existing disturbances and development. In partitioning the tendencies, we note that, for example, the local change in the u-component of the wind caused by a moving weather system is

$$\frac{\partial u}{\partial t} = - c \cdot \nabla u + \frac{du}{dt} \qquad (18)$$

where c is the velocity of an advective or steering current (Fjortoft,1952), usually a smoothed middle tropospheric wind. Let $u=u_0+u'$ where $u_0$ is the u-component of the steady state part of the circulation and u' is the u-component arising from development. Then,

$$\frac{\partial u}{\partial t} = - c \cdot \nabla u_o + \left(\frac{du'}{dt} - c \cdot \nabla u'\right) \qquad (19)$$

The first term of (19) is the local change in u caused by translation of the steady state part of the weather disturbance. The second term contains the local change of u from development. Note that the vertical advection of u is considered part of development.

The use of the advective current throughout the troposphere is valid because most synoptic systems tend to maintain vertical structure. Any changes in vertical structure are assumed to be the result of development. The variational formalism requires that the adjustments be carried out on the total velocity components. Therefore, we represent the local tendency of u by (18). The total derivative, an approximate developmental component, is defined as a new dependent variable, $\varepsilon_u = du/dt$ ($\varepsilon_v = dv/dt$).

d) Transformation of the Integrated Continuity Equation

The mass continuity equation in generalized coordinates (Shuman and Hovermale, 1968) is

$$\frac{\partial}{\partial t}\left(\frac{\partial p}{\partial \sigma}\right) + \frac{\partial}{\partial \sigma}\left(\dot{\sigma}\frac{\partial p}{\partial \sigma}\right) + m\left[\frac{\partial}{\partial x}\left(u\frac{\partial p}{\partial \sigma}\right) + \frac{\partial}{\partial y}\left(v\frac{\partial p}{\partial \sigma}\right)\right] - \frac{\partial p}{\partial \sigma}\left(u\frac{\partial m}{\partial x} + v\frac{\partial m}{\partial y}\right) = 0 \qquad (20)$$

The material derivative in the Lambert map projection is

$$\frac{d}{dt} = \frac{\partial}{\partial t} + mu\frac{\partial}{\partial x} + mv\frac{\partial}{\partial y} + \dot{\sigma}\frac{\partial}{\partial \sigma} \qquad (21)$$

Upon expanding the map scale factor m, (20) becomes

$$\nabla_3 \cdot \vec{V} + R_1 K^2 \left(\frac{\partial u/K}{\partial x} + \frac{\partial v/K}{\partial y}\right) + \frac{d}{dt}\left(\ell n \frac{\partial p}{\partial \sigma}\right) = 0 \qquad (22)$$

The last term of (22) is determined from the nonlinear vertical coordinate (5). Further, given (6) and the following definitions,

$$\alpha = \sigma^*/(p^*-p_u), \tag{23}$$

$$J = 3\beta\,(p-p^*)^3 + \alpha\,(p-p^*), \tag{24}$$

it can be shown that

$$\frac{d}{dt}(\ell n\,\frac{\partial p}{\partial \sigma}) = q_1\,\dot{\sigma} + q_2\,\omega_s \tag{25}$$

$$\text{if} \qquad q_1 = \frac{-2[J-\alpha\,(p-p^*)]}{J^2} \tag{26}$$

$$q_2 = \frac{(p-p^*)^3}{(p_s-p^*)4}\;\frac{J_s\,[J\;2\alpha\,(p-p^*)]}{J^2} \tag{27}$$

$J_s$ is obtained by substituting $p_s$ for p in (24). Including these modifications leads to the following form for the continuity equation,

$$\frac{\partial u}{\partial x} + \frac{\partial v}{\partial y} + \frac{\partial \dot{\sigma}}{\partial \sigma} + q_1\,\dot{\sigma} + F = 0 \tag{28}$$

$$\text{where} \qquad F = q_2\,\omega_s + R_1K^2\,(\frac{\partial u/K}{\partial x} + \frac{\partial v/K}{\partial y}) \tag{29}$$

The $q_1$ and $q_2$ arise through the nonlinearity of the coordinate transformation. They vanish where $p \geq p^*$.

When solved for the vertical velocity, (28) becomes,

$$\dot{\sigma} = \dot{\sigma}_o Q_o - \int_{\sigma_o}^{\sigma_1} H\,Q\,d\sigma \tag{30}$$

where

$$H = \frac{\partial u}{\partial x} + \frac{\partial v}{\partial y} + F \tag{31}$$

and

$$Q = e^{-\int_{\sigma}^{\sigma_1} q_1\,d\sigma} \tag{32}$$

The integral function, Q, is proportional to the pressure thickness of the sigma layers. In order to simplify the Euler-Lagrange equations derived in the following section, we require Q=1. This assumption removes the dependence of the integrated divergence on the variable pressure thickness of the sigma layers. Therefore, divergences in the layers near the surface over elevated terrain receive proportionally greater weight in the vertical velocity adjustment.

e) Finite Difference Equations for the Dynamic Constraints

Two variational models were derived with finite difference versions of the dynamic constraints. The first was derived with the dynamic equations written in uncentered differences on a uniform grid and the second was formulated with centered differences on a staggered grid. We sought difference formulations for the Euler-Lagrange equations that were symmetric about the central grid point. The centered difference formulation on a staggered grid proved most suitable from this standpoint.

Shuman and Hovermale (1968) and Anthes and Warner (1978) define the horizontal finite difference operators and the finite averaging operators as

$$\alpha_x \equiv (\alpha_{i+1/2,j} - \alpha_{i-1/2,j}) \; / \; \Delta x$$

$$\alpha_y \equiv (\alpha_{i,j+1/2} - \alpha_{i,j-1/2}) \; / \; \Delta y$$

$$\bar{\alpha}^x \equiv (\alpha_{i+1/2,j} + \alpha_{i-1/2,j}) \; / \; 2 \qquad (33)$$

$$\bar{\alpha}^y \equiv (\alpha_{i,j+1/2} + \alpha_{i,j-1/2}) \; / \; 2$$

The i is the east-west index, the j is the north-south index as measured at the grid origin which is located at the lower left corner of the grid. In addition, the vertical differences and averages are defined by

$$\alpha_\sigma \equiv (\alpha_{k+1/2} - \alpha_{k-1/2}) \; / \; \Delta\sigma$$

$$\overline{\alpha}^{\sigma} \equiv (\alpha_{k+1/2} + \alpha_{k-1/2}) \; / \; 2 \qquad (34)$$

Figure 4 shows the staggered grid developed for this model. The geopotential $\Phi$ is defined at the grid intersections, v is located at the top and bottom and u is located at the sides of the grid square. The divergence D is found at the center of the grid. The layer mean temperatures T are defined at one half grid length above and below the grid intersections and the vertical velocity, $\dot{\sigma}$, is located one half grid space above and below the divergence. Mesinger and Arakawa (1976) have shown that phase speed and dispersion properties of this staggered grid make it inferior relative to other grid configurations for numerical prediction. However, the grid with v located on the top and bottom and u located on the sides of the grid box is well suited for the solution sequence developed for the Euler-Lagrange equations in the following section. Other variables used in the variational analysis are collocated with the variables in Fig. 4 as follows: $\varepsilon_v$ and $\lambda_1$ at v, $\varepsilon_u$ and $\lambda_2$ at u, $\lambda_3$ at D, and $\lambda_4$ at T.

The finite difference equations for the horizontal momentum equations written for the staggered grid are

$$M_1 = R_o[\overline{\varepsilon_u}^{xy} + \overline{m}^{x}\overline{(u - c_x)}^{xy}\,\overline{u_x}^{y} + \overline{m}^{x}(v - c_y)\,\overline{u_y}^{x} + R_o\,\overline{\dot{\sigma}}^{y\sigma}\,\overline{u}^{xy\sigma}]$$
$$- (1+R_1\overline{C}^{x})v + (1+R_1\overline{K}^{x})\,[\phi_x + (\Delta T\,\ell n\, p/p_\sigma)_x] + f_u = 0 \qquad (35)$$

$$M_2 = R_o \left[\overline{\varepsilon}_v^{xy} + \overline{m}^y (u - c_x)\ \overline{v}_x^y + \overline{m}^y \overline{(v - c_y)}^{xy}\ \overline{v}_y^x + R_o\ \dot{\overline{\sigma}}^{x\sigma}\ \overline{v}_\sigma^{xy\sigma}\right]$$

$$+ (1+R_1\overline{C}^y)u + (1+R_1\overline{K}^y)\ [\phi_y + (\Delta T\ \ell n\ p/p_\sigma)y] + f_v = 0 \qquad (36)$$

The analogues for the continuity and hydrostatic equations are

$$M_3 = \int (u_x + v_y)\ d\sigma + (\dot{\sigma} - \dot{\sigma}_o\ e^{-\overline{q}_1 \int d\sigma}) + \int \left[\frac{Lh}{H\ell}\ q_2 \omega_s + R_1 \overline{K}^{xy}(u_x + v_y)\right.$$

$$\left. -R_1(\overline{u}^x\ \overline{K}_x^y + \overline{v}^y\ \overline{K}_y^x)\right]\ d\sigma = 0 \qquad (37)$$

$$M_4 = \phi_\sigma + \overline{T}^\sigma\ (\ell n\ p)_\sigma + (\Delta T\ \ell n\ p/p_\sigma)_\sigma = 0 \qquad (38)$$

The four dynamic constraints are referenced, respectively, to the following locations: $M_1$ at v, $M_2$ at u, $M_3$ at D, and $M_4$ at T on Fig. 4.

## 4. Euler-Lagrange Equations

The variational analysis melds satellite data with conventional data at the second stage of a two-stage objective analysis. All data are gridded independently in the first stage and are combined in the second stage. Future versions will combine the two stages. The gridded observations to be modified are meshed with the dynamic constraints through Sasaki's (1970a) variational formulation. The finite difference analog of the adjustment functional is

$$\tilde{F} = \Delta x \Delta y \sum_i \sum_j a_i b_j\ I_{ij} \qquad (39)$$

The integrand $I_{i,j}$ is

$$I = \pi_1\ (u-u^o)^2 + \pi_1\ (v-v^o)^2 + \pi_2\ (\dot{\sigma}-\dot{\sigma}^o)^2 + \pi_3\ (\phi-\phi^o)^2$$

$$+ \pi_4\ (\overline{T}-\overline{T}^o)^2 + \pi_5\ (\phi_x - \phi_x{}^o)^2 + \pi_5\ (\phi_y - \phi_y{}^o)^2 + \pi_6\ (\phi_\sigma - \phi_\sigma{}^o)^2$$

$$+ \pi_7 (\xi_u - \xi_u^o)^2 + \pi_7 (\xi_v - \xi_v^o)^2 + 2\lambda_1 M_1 + 2 \lambda_2 M_2 + 2 \lambda_3 M_3$$

$$+ 2 \lambda_4 M_4 \qquad (40)$$

The weights $\pi_i$, i=1,7 are Gauss' precision moduli (Whittaker and Robinson, 1926). The gridded observations ($u^o$, $v^o$, $\dot{\sigma}^o$, $\Phi^o$, $\bar{T}^o$, $\varepsilon_u{}^o$, $\varepsilon_v{}^o$) to be adjusted enter in a least squares formulation and receive precision modulus weights according to their relative observation accuracies. The strong constraints to be satisfied exactly are introduced through the Lagrangian multipliers $\lambda_i$, i=1,4.

Objectively modified meteorological variables are determined by requiring the first variation on F to vanish. A necessary condition for the existence of a stationary set is that the functions are determined from the domain of admissible functions as solutions of the Euler-Lagrange equations. The variation is to be carried out at every point (r,s) within the grid. Thus, setting the weights $a_i = b_j = 1$ and differentiating the integrand (40) with respect to the arbitrary variable $(\alpha_{r,s})$, the Euler-Lagrange operator in finite differences is

$$\frac{\partial I_{i,j}}{\partial \alpha_{r,s}} = I_{\alpha_{i,j}} \frac{\partial \alpha_{i,j}}{\partial \alpha_{r,s}} = I_{\alpha_{i,j}} \delta_r^i \delta_s^j = 0 \qquad (41)$$

The delta functions $\delta_r^i$, $\delta_s^j$, equal 1 where r=i or s=j and are zero elsewhere. Each term in $I_{i,j}$ that contains an overbar term, e.g. $\bar{\alpha}^x_{r,s}$, produces a corresponding overbar term in the Euler-Lagrange equations when subjected to the operations specified by (41). It is convenient that the multiplicate overbar terms such as $\bar{\alpha}^{xy}_{r,s}$ that appear in the nonlinear terms of the constraints be replaced by $\alpha_{r,s}$ so that fewer gridpoints are required to express these terms in the Euler-Lagrange equations.

The Euler-Lagrange equations for u, v, and $\dot{\sigma}$ result from the operations specified by (41). The equations are

$$\Pi_1 (u-u^o) - (\int d\sigma)\, \lambda_{3x} + \lambda_2 (1+R_1\bar{C}^y) + R_o \{\bar{m}^y \bar{\lambda}_1^{xy} \bar{u}_x^x + \bar{m}^y \lambda_2 \bar{v}_x^y - [\bar{m}^{xy}\bar{\lambda}_1^y (\overline{u-c_x})^x]_x - [m \overline{\lambda_1 (v-c_y)^x}]_y - R_o (\dot{\bar{\sigma}}^x \bar{\lambda}_1^{xy\sigma})_\sigma\} - R_1 [(\lambda_3 \bar{K}^{xy})_x + \lambda_3 \bar{K}_x^{xy}] = 0 \quad (42)$$

$$\Pi_1 (v-v^o) - (\int d\sigma)\, \lambda_{3y} - \lambda_1 (1+R_1\bar{C}^x) + R_o \{\bar{m}^x \lambda_1 \bar{u}_y^x + \bar{m}^x \bar{\lambda}_2^{xy} \bar{v}_y^y - [m \overline{\lambda_2 (u-c_x)^y}]_x - [\bar{m}^{xy}\bar{\lambda}_2^x \overline{(v-c_y)^y}]_y - R_o (\dot{\bar{\sigma}}^y \bar{\lambda}_2^{xy\sigma})_\sigma\} - R_1 [(\lambda_3 \bar{K}^{xy})_y + \lambda_3 \bar{K}_y^{xy}] = 0 \quad (43)$$

$$\Pi_2 (\dot{\sigma} - \dot{\sigma}^o) + \bar{\lambda}_3^\sigma + R_o^2 [\bar{\lambda}_1^{y\sigma} \bar{u}_\sigma^x + \bar{\lambda}_2^{x\sigma} \bar{v}_\sigma^y] = 0 \quad (44)$$

The Euler-Lagrange equations for the thermodynamic variables $\Phi$ and $\bar{T}$ are

$$\bar{\Pi}_5^x (\phi-\phi^o)_{xx} + \bar{\Pi}_5^y (\phi-\phi^o)_{yy} + \bar{\Pi}_6^\sigma (\phi-\phi^o)_{\sigma\sigma} + \Pi_{5x} (\bar{\phi}_x^x - \bar{\phi}_x^{o\,x}) + \Pi_{5y} (\bar{\phi}_y^y - \bar{\phi}_y^{o\,y}) + \Pi_{6\sigma} (\bar{\phi}_\sigma^\sigma - \bar{\phi}_\sigma^{o\,\sigma}) - \Pi_3 (\phi-\phi^o) + \lambda_{1x} (1+R_1K) + \lambda_{2y} (1+R_1K) + \lambda_{4\sigma} = 0 \quad (45)$$

$$\Pi_4 (\bar{T}^\sigma - \bar{T}^{o\,\sigma}) + \gamma\lambda_4 = 0 \quad (46)$$

Similarly, the operations performed for $\varepsilon_u$ and $\varepsilon_v$ yield

$$\Pi_7 (\varepsilon_u - \varepsilon_u^o) + R_o \bar{\lambda}_1^{xy} = 0 \quad (47)$$

$$\Pi_7 (\varepsilon_v - \varepsilon_v^o) + R_o \bar{\lambda}_2^{xy} = 0 \quad (48)$$

Variation on the Lagrange multipliers restores the four original dynamic constraints (35)-(38).

Some of these Euler-Lagrange equations are complicated nonlinear partial differential equations for which solutions are difficult to obtain by direct methods. We observe, however, that the nonlinear terms are all products with the Rossby number or with $R_1$. These equations may therefore be linearized and a solution obtained through a cyclical method as follows. Terms multiplied by $R_o$ or $R_1$ are expressed with observed variables at the first cycle, and are expressed by previously adjusted variables at higher cycles. At any particular solution cycle, these terms and the terms that are determined by observed variables are specified and can be treated as forcing functions. We emphasize that this solution method is valid only for the latitudes and scales of motion where the Rossby number is less than one.

Upon linearization, the Euler-Lagrange equations for u, v, $\dot{\sigma}$, and $\Phi$ become

$$\Pi_1 u - (\Delta\sigma)\,\lambda_{3x} + \lambda_2 + F_1 = 0 \tag{49}$$

$$\Pi_1 v - (\Delta\sigma)\,\lambda_{3y} - \lambda_1 + F_2 = 0 \tag{50}$$

$$\Pi_2\dot{\sigma} + \overline{\lambda_3}^{\sigma} + F_3 = 0 \tag{51}$$

$$\overline{\Pi_5}^{x}\,\phi_{xx} + \overline{\Pi_5}^{y}\,\phi_{yy} + \overline{\Pi_6}^{\sigma}\,\phi_{\sigma\sigma} + \Pi_{5x}\overline{\phi}^{x}_{x} + \Pi_{5y}\overline{\phi}^{y}_{y} + \Pi_{6\sigma}\overline{\phi}^{\sigma}_{\sigma}$$

$$- \Pi_3\phi + \lambda_{1x} + \lambda_{2y} + \lambda_{4\sigma} + F_4 = 0 \tag{52}$$

Similarly, the four dynamic constraints become

$$\phi_x - v + F_5 = 0 \tag{53}$$

$$\phi_y + u + F_6 = 0 \tag{54}$$

$$\int (u_x + v_y)\, d\sigma + \dot{\sigma} + \Delta\sigma\, F_7 = 0 \tag{55}$$

$$\phi_\sigma + \gamma\overline{T}^{\sigma} + \beta = 0 \tag{56}$$

Now these equations and (46)-(48) complete a set of eleven simple algebraic or linear partial differential equations. Variables may be easily eliminated to reduce the number of equations. Equations (49), (50), (53), and (54) formulated as vorticity expressions are combined to eliminate u and v.

$$\lambda_{1x} + \lambda_{2y} = (\Pi_1\phi_x)_x + (\Pi_1\phi_y)_y - F_{1y} + F_{2x} + (\Pi_1 F_5)_x + (\Pi_1 F_6)_x \tag{57}$$

Equation (56) is combined with (46) to eliminate $\overline{T}$,

$$\lambda_{4\sigma} = \left(\frac{\Pi_4}{\gamma^2}\,\phi_\sigma\right)_\sigma + F_8 \tag{58}$$

where

$$F_8 = \left(\frac{\Pi_4}{\gamma}\,\overline{T}^{-\sigma}_{o}\right)_\sigma + \left(\frac{\Pi_4\beta}{\gamma^2}\right)_\sigma \tag{59}$$

Note that both (57) and (58) contain terms that obey the identity

$$(AB_z)_z = \overline{A}^{z} B_{zz} + A_z \overline{B}^{z}_{z} \tag{60}$$

Now $\lambda_1$, $\lambda_2$, and $\lambda_4$ can be eliminated in (52), (57), and (58). This leaves a three-dimensional second-order partial differential equation with non-constant coefficients in $\Phi$;

$$(\overline{\Pi}_1^x + \overline{\Pi}_5^x)\ \phi_{xx} + (\overline{\Pi}_1^y + \overline{\Pi}_5^y)\ \phi_{yy} + (\overline{\Pi}_6^\sigma + (\frac{\overline{\Pi}_4^\sigma}{\gamma^2}))\ \phi_{\sigma\sigma} + (\Pi_1 + \Pi_5)_x\ \overline{\phi}_x^x$$

$$+ (\Pi_1 + \Pi_5)_y\ \overline{\phi}_y^y + (\Pi_6 + \frac{\Pi_4}{\gamma^2})_\sigma\ \overline{\phi}_\sigma^\sigma - \Pi_3\phi + F_9 = 0 \qquad (61)$$

where

$$F_9 = - F_{1y} + F_{2x} + (\Pi_1 F_5)_x + (\Pi_1 F_6)_y + F_4 + F_8 \qquad (62)$$

All of the coefficients of the geopotential and its derivatives are functions of sums and/or derivatives of precision modulus weights. The coefficients of the three second order partial derivatives are sums of precision moduli. These are always positive because the precision moduli are always positive. Thus (61) must be everywhere elliptic.

We also derive a diagnostic equation in $\lambda_3$. First, (49) and (50) are divided by $\pi_1$ and reformulated as components of the divergence. Then they are combined into the divergence and integrated in the vertical to yield,

$$- \int (u_x + v_y)\ d\sigma + (\lambda_{3x} \int \frac{\int d\sigma}{\Pi_1}\ d\sigma)_x + (\lambda_{3y} \int \frac{\int d\sigma}{\Pi_1}\ d\sigma)_y$$

$$- \int \{[\ \frac{1}{\Pi_1}\ (\lambda_2 + F_1)\ ]_x - [\frac{1}{\Pi_1}\ (-\lambda_1 + F_2)]_y\}\ d\sigma = 0 \qquad (63)$$

Now $\dot{\sigma}$ is eliminated from (51) and (55) and the result replaces the integrated divergence in (63). Application of the identity (60) to several terms of (63) yields the two-dimensional second-order elliptic partial differential equation for $\lambda_3$,

$$\int \left(\frac{\overline{\int d\sigma}^{x}}{\Pi_1}\right) d\sigma \; \lambda_{3xx} + \int \left(\frac{\overline{\int d\sigma}^{y}}{\Pi_1}\right) d\sigma \; \lambda_{3yy} + \overline{\lambda}^{x}_{3x} \int \left(\frac{\int d\sigma}{\Pi_1}\right)_x d\sigma$$

$$+ \overline{\lambda}^{y}_{3y} \int \left(\frac{\int d\sigma}{\Pi_1}\right)_y d\sigma - \frac{\lambda_3}{\Pi_2} + F_{10} = 0 \qquad (64)$$

where

$$F_{10} = - \int \left\{\left[\frac{1}{\Pi_1}(\lambda_2 + F_1)\right]_x + \left[\frac{1}{\Pi_1}(-\lambda_1 + F_2)\right]_y\right\} d\sigma - \frac{F_3}{\Pi_2} + F_7$$

The relationship between u, v, and $\lambda_3$ in (49) and (50) shows $\lambda_3$ is an adjustment velocity potential. Equation (64) must be solved for the adjustment velocity potential. With the exception of a few small terms that contain the divergent part of the wind, (61) is a diagnostic equation for the rotational part of the wind. All other dependent variables can be calculated once $\Phi$ and $\lambda_3$ have been determined. The solution sequence requires that the divergent components enter the velocity components, calculated from (53) and (54), through forcing functions that depend upon "old" data. In order for the divergent part of the wind to be current with the rotational part of the wind, the adjusted wind components are first found through (53) and (54) and these are readjusted for the divergent part of the wind. This solution method is not strictly rigorous, requiring an adjustment of an adjustment. Its verification through a case study is the subject of the accompanying paper.

## 5. Computational Details

The ten level variational assimilation model has the state variables staggered in both the horizontal and vertical dimensions. See Fig. 4 for the horizontal grid template. The variables u, v, $\varepsilon_u$, $\varepsilon_v$, and $\Phi$ are located at 100 mb intervals from the top of the domain (100 mb) to 700 mb ($p^*$). The constraints $M_1$, $M_2$, and $M_3$ are referenced to these surfaces. $\overline{T}$, $\dot{\sigma}$, and $M_4$ appear at 150-, 250-, 350-, 450-, 550-, and 650-mb surfaces. Further, the

upper boundary on $\dot{\sigma}$ is at 50 mb ($\dot{\sigma}$=0). Below $p^*$, u, v and the developmental components appear on sigma surfaces and $\dot{\sigma}$ and $M_4$ are located at the half levels. The first three dynamic constraints and $\Phi$ are referenced to the equivalent pressure levels and the mean layer temperature is located at the half levels. The lower boundary for $\dot{\sigma}$ ($\dot{\sigma}$=0) is the ground. We have also chosen the surface observations to be representative of the average conditions of the lowest sigma layer. This means that the boundary layer divergence is representative of the mean divergence of this lowest layer.

The correct number of boundary conditions are furnished by the variational formulation such that a unique solution is provided when natural and/or imposed boundary equations are satisfied (Forsythe and Wasow, 1960). Natural boundary conditions are derived from the constraints as numerical expressions to be solved. However, because the MODEL I dynamic constraints produce complex boundary conditions, we use imposed boundary conditions and specify the dependent variables on the boundaries. The requirements of the solution method for MODEL I are that boundary conditions be specified for the geopotential and adjustment velocity potential diagnostic equations, the remaining equations in the adjustment cycle, and the vertical velocity. In addition, special boundary conditions are imposed by the cyclic solution sequence. Details of the various boundary conditions follow.

a) Boundary Conditions on the Geopotential Adjustment

Imposed boundary conditions for the geopotential adjustment equation (61) are supplied by the gridded fields of the observed meteorological component of the partitioned height field. The top boundary is provided by the analysis at

100 mb. The lower boundary is the meteorological height component transformed onto equivalent pressure surfaces.

b) Boundary Conditions on the Velocity Adjustment Potential

Lateral boundary conditions are required for the adjustment velocity potential equation (64). It is well known that the specification of boundary conditions on the velocity potential determines the structural details of the recovered wind field to some degree (Hawkins and Rosenthal, 1965). Furthermore, there appears to be no method of uniquely specifying the boundary conditions (Shukla and Saha, 1974; Eskridge, 1977; Liu, 1977, Stephens and Johnson, 1978). Dirichlet boundary conditions force all of the divergence adjustment into the v-component along the x-boundaries and into the u-component along the y-boundaries. Neumann boundary conditions force the adjustment into the u-component along the x-boundaries and into the v-component along the y-boundaries. We used Dirichlet conditions and set the adjustment velocity potential equal to zero on all boundaries. This choice for boundary conditions left the divergent part of the wind unadjusted at the boundaries.

c) Boundary Conditions on the Vertical Velocity

The boundary conditions on $\dot{\sigma}$ are $\dot{\sigma}=0$ at the ground and at 50 mb. Because the lower coordinate surface slopes with the underlying terrain, there may exist vertical velocity near the ground. Given as $\omega_s=dp_s/dt$, the surface vertical velocity is a combination of flow over elevated terrain and through evolving meteorological pressure fields. Upon partitioning into terrain and

meteorological components, the surface vertical velocity is

$$\omega_s = - (V \cdot \nabla p_T + \frac{\partial p_m}{\partial t} + V \cdot \nabla p_m) \qquad (65)$$

Scale analysis of the terms of (65) showed the first term in parentheses to be at least an order of magnitude larger than the meteorological terms. We therefore approximated the surface vertical velocity with the first term.

d) Boundary Conditions on the Remaining Variables

Horizontal boundary conditions are not required to determine the remaining variables in the interior of the analysis domain. However, boundary values of these variables are required in order to calculate horizontal derivatives for the forcing functions in subsequent solution cycles. Interior fields are extrapolated across the boundaries by using an approximation that is the sum of a locally averaged curvature with one half of a locally averaged gradient. This method provides boundaries that are compatible with the adjusted fields; they are generated, however, to eliminate boundary discontinuities, and do not satisfy the dynamic equations.

e) Boundary Conditions Required by the Cyclic Solution Method

Initial tests of the variational assimilation model with the case study described in the following article (Achtemeier, et al., 1988) revealed local violations of linear stability along the lateral boundaries. These instabilities spread into the interior of the model domain with successive cycles. The adjustment of the geopotential height field (61) is forced to take on the gridded values of the observed geopotential at the boundaries

regardless of the relative weights ascribed to the other variables. Small perturbations in the heights near the boundaries are frozen into the geopotential adjustment and cause the instabilities. We were unable to totally eliminate the perturbations but were able to eliminate the buildup of the undesired waves by requiring variational analysis to satisfy the geostrophic, hydrostatic equations near the boundaries. These solutions grade into the solutions for the full nonlinear dynamic equations at five grid spaces into the grid interior.

f) Convergence Criteria

The convergence criteria for the general second-order partial differential equation with nonconstant coefficients,

$$a\lambda_{xx} + b\lambda_{yy} + c\lambda_{\sigma\sigma} + d\lambda_{x} + e\lambda_{y} + f\lambda_{\sigma} - g\lambda + h = 0 \qquad (66)$$

obtained by the partial wave technique is

$$\left( \frac{a}{\Delta x^2} + \frac{b}{\Delta y^2} + \frac{c}{\Delta \sigma^2} + \frac{g}{2} \right)^2 > \left( \frac{d}{\Delta x} + \frac{e}{\Delta y} + \frac{f}{\Delta \sigma} \right)^2 \qquad (67)$$

The coefficients a, b, c, and g in the geopotential adjustment equation are always positive. Further, the coefficient d is just the horizontal derivative of a, e is the horizontal derivative of b, and f is the vertical derivative of c. The most stringent convergence requirement is that the absolute magnitude of the derivative of a coefficient not exceed the value of the coefficient. This requirement can be easily satisfied through the definitions of the precision modulus weights. The coefficients of the adjustment velocity potential are similarly related except that c=f=0.

Convergence of the cyclic solution sequence for MODEL I is assured for the latitudes and scales of motion where the Rossby number is less than one. When the Rossby number exceeds one, the adjustment terms in the forcing functions approach or exceed the magnitudes of the variables being solved for, a condition that favors the development of linear instability. A determination of the limits of convergence MODEL I is the subject of continuing research.

## 6. Some Concluding Remarks

We have presented an outline of the first of four variational assimilation models that will meld data collected from rawinsonde (wind, temperature, height, moisture) with data collected from space-based platforms (cloud wind vectors, moisture, mean-layer temperatures). This method is, by design, independent of numerical prediction models. The first model, MODEL I, incorporates as dynamical constraints, the two nonlinear horizontal momentum equations, the hydrostatic equation, and an integrated continuity equation. The vertical coordinate minimizes the interpolation from pressure to terrain-following coordinates, more easily accommodating mean-layer temperature data observed by satellite in the middle and upper troposphere, and decreases truncation error associated with the pressure gradient force in the horizontal momentum equations. Reformulations for the horizontal tendencies of u and v are designed to increase the accuracy of the variational analysis for these hypersensitive quantities.

We designed a cyclical solution sequence that linearizes the eleven Euler-Lagrange equations that comprise MODEL I as functions of the Rossby

number. This solution method does not exclude ageostrophic motion, it only requires that the Rossby number be less than one. A potential problem in the calculation of the adjusted velocity components is that this solution method is not strictly rigorous, requiring an adjustment of an adjustment. Its verification through a case study is the subject of the following paper (Achtemeier et al., 1988).

## Acknowledgements

This research was supported by the National Aeronautics and Space Administration (NASA) under contract NAS8-34902 and grant NAG8-059. We gratefully acknowledge Mrs. Julia Chen for her monumental programming effort.

REFERENCES

Achtemeier, G. L., 1975: On the Initialization problem: A variational adjustment method. Mon. Wea. Rev., 103, 1090-1103.

_____, 1979: Evaluation of a variational initialization method. Preprints, 4th Conf. Num. Wea. Pred., Amer. Meteor. Soc. 1979, 1-8.

_____, S. Q. Kidder and R. W. Scott, 1988: A multivariate variational objective analysis - assimilation method, Part II: Case study results with and without satellite data. (Submitted to Tellus)

Anthes, R. A., and T. T. Warner, 1978: Development of hydrodynamic models suitable for air pollution and other mesometeorological studies. Mon. Wea. Rev., 106, 1045-1078.

Baer, F., and J. Tribbia, 1977: On complete filtering of gravity modes through nonlinear initialization. Mon. Wea. Rev., 105, 1536-1539.

Baker, W. E., 1983: Objective analysis and assimilation of observational data from FGGE. Mon. Wea. Rev., 111, 328-342.

Bengtsson, L., M. Kanamitsu, P. Kallberg and S. Uppala, 1982: FGGE 4-dimensional data assimilation at ECMWF. Bull. Amer. Meteor. Soc., 63, 29-43.

Bloom, S. C., 1983: The use of dynamical constraints in the analysis of mesoscale rawinsonde data. Tellus, 35, 363-378.

Bratseth, A. M., 1986: Statistical interpolation by means of successive corrections. Tellus, 38A, 439-447.

Charney, J. G., 1948: On the scale of atmospheric motion. Geofys. Publikas., 17, 1-17.

Courant, R., 1936: Differential and Integral Calculus, Vol. 2, (E. J. McShane, translator), Wiley - Interscience, p198.

Cressman, G. P., 1959: An operational objective analysis system. Mon. Wea. Rev., 87, 367-374.

Daley, R., 1981: Normal mode initialization. Reviews of Geophysics and Space Physics, 19, 450-468.

Eskridge, R. E., 1977: Comments on "An iterative algorithm for objective wind field analysis." Mon. Wea. Rev., 105, 1066.

Fjortoft, R., 1952: On a numerical method of integrating the barotropic vorticity equation. Tellus, 4, 179-194.

Forsythe, G. E., and W. R. Wasow, 1960: Finite Difference Methods for Partial Differential Equations. New York, John Wiley and Sons.

Gandin, L. S., 1963: Objective analysis of meteorological fields. Isdat., Leningrad. [Israel Program for Scientific Translations, Jerusalem, 1965, 242 pp.]

Ghil, M., M. Halem and R. Atlas, 1979: Time-continuous assimilation of remote-sounding data and its effect on weather forecasting. Mon. Wea. Rev., 107, 140-171.

Haltiner, G. J., 1971: Numerical Weather Prediction, Wiley and Sons, USA, 46-61.

Hawkins, H. F., and S. L. Rosenthal, 1965: On the computation of stream functions from the wind field. Mon. Wea. Rev., 93, 245-252.

Ikawa, M., 1984: An alternative method of solving weak constraint problem and a unified expression of weak and strong constraints in variational objective analysis. Pap. Meteor. & Geophys., 35, 71-80.

Krishnamurti, T. N., 1968: A diagnostic balance model for studies of weather systems of low and high latitudes. Rossby number less than one. Mon. Wea. Rev., 96, 197-207.

Lewis, J. M., 1980: Dynamical adjustment of 500 mb vorticity using P.D. Thompson's scheme - a case study. Tellus, 32, 511-514.

_____, and J. C. Derber, 1985: The use of adjoint equations to solve a variational adjustment problem with advective constraints. Tellus, 37A, 309-322.

_____, 1982: Adaptation of P.D. Thompson's scheme to the constraint of potential vorticity conservation. Mon. Wea. Rev., 110, 1618-1634.

_____, and T.H. Grayson, 1972: The adjustment of surface wind and pressure by Sasaki's variational matching technique. J. Appl. Meteor., 11, 586-597.

_____, C. M. Hayden and A. J. Schreiner, 1983: Adjustment of VAS and RAOB geopotential analysis using quasi-geostrophic constraints. Mon. Wea. Rev., 111, 2058-2067.

Liu, C. Y., 1977: Reply. Mon. Wea. Rev., 105, 1067.

Machenhaur, B., 1977: On the dynamics of gravity oscillations in a shallow water model, with applications to normal mode initialization. Beitr. Phys. Atmos., 50, 253-271.

McPherson, R. D., K. H. Bergman, R. E. Kistler, G. E. Rasch, and D. S. Gorden, 1979: The NMC operational global data assimilation system. Mon. Wea. Rev., 107, 1445-1461.

Mesinger, F., and A. Arakawa, 1976: Numerical methods used in atmospheric models. Vol. 1, GARP Publications Series No. 17, p47.

Miyakoda, K., and R. M. Moyer, 1968: A method of initialization for dynamical

weather forecasting. Tellus, 20, 115-130.

Nitta, T., and J. B. Hovermale, 1969: A technique of objective analysis and initialization for the primitive forecast equations. Mon. Wea. Rev., 97, 652-658.

O'Brien, J. J., 1970: Alternative solutions to the classical vertical velocity problem. J. Appl. Meteor., 9, 197-203.

Phillips, N. A., 1957: A coordinate system having some special advantages for numerical forecasting. J. Meteor., 14, 184-195.

Sasaki, Y., 1958: An objective analysis based upon the variational method. J. Meteor. Soc. Japan, 36, 77-88.

_____, 1970a: Some basic formalisms in numerical variational analysis. Mon. Wea. Rev., 98, 875-883.

_____, 1970b: Numerical variational analysis formulated under the constraints as determined by longwave equations and a low-pass filter. Mon. Wea. Rev., 98, 884-898.

_____, and Lewis, J., 1970: Numerical variational analysis of the planetary boundary layer in conjunction with squall line formation. J. Meteor. Soc. Japan, 48, 381-398.

Schlatter, T. W., 1975: Some experiments with a multivariate statistical objective analysis scheme. Mon. Wea. Rev., 103, 246-257.

Shukla, J., and K. R. Saha, 1974: Computation of non-divergence streamfunction and irrotational velocity potential from the observed winds. Mon. Wea. Rev., 102, 419-425.

Shuman, F., and J. B. Hovermale, 1968: An operational six-layer primitive equation model. J. Appl. Meteor., 7, 525-547.

Smith P. J., and C. P. Lin, 1978: A comparison of synoptic scale vertical motions computed by the kinematic method and two forms of the omega equation. Mon. Wea. Rev., 106, 1687-1694.

Stephens, J. J., and K. W. Johnson, 1978: Rotational and divergent wind potentials. Mon. Wea. Rev., 106, 1452-1457.

Temperton, C., 1984: Variational normal mode initialization for a multilevel model. Mon. Wea. Rev., 112, 2303-2316.

Thompson, P. D., 1969: Reduction of analysis error through constraints of dynamical consistency. J. Appl. Meteor., 9, 738-742.

Wahba, G., and J. Wendelberger, 1980: Some new mathematical methods for variational objective analysis using splines and cross validation. Mon. Wea. Rev., 108, 1122-1143.

Wang, P. K., 1984: A brief review of the Eulerian variational principle for

atmospheric motions in rotating coordinates. Atmos.-Ocean, 22, 387-392.

Whittaker, E., and G. Robinson, 1926: The Calculus of Observations (2nd Edition). London, Blackie and Son, LTD., p176.

Williamson, D. L., and R. Daley, 1983: An iterative analysis initialization technique. Mon. Wea. Rev., 111, 1517-1536.

## Figure Captions

Figure 1. The relationship between sigma and pressure for the levels below the elevation of the 600 mb pressure surface for the coordinate parameters that have been selected for the variational objective analysis.

Figure 2. The distribution of hybrid coordinate surfaces below 600 mb as the surface pressure varies from 800 to 1025 mb.

Figure 3. Heights at the lower coordinate surface for a) nonpartitioned terrain-following coordinate, b) the 1000 mb pressure surface, and c) the equivalent pressure surface.

Figure 4. A portion of the staggered grid used for the variational diagnostic model.

Fig 1

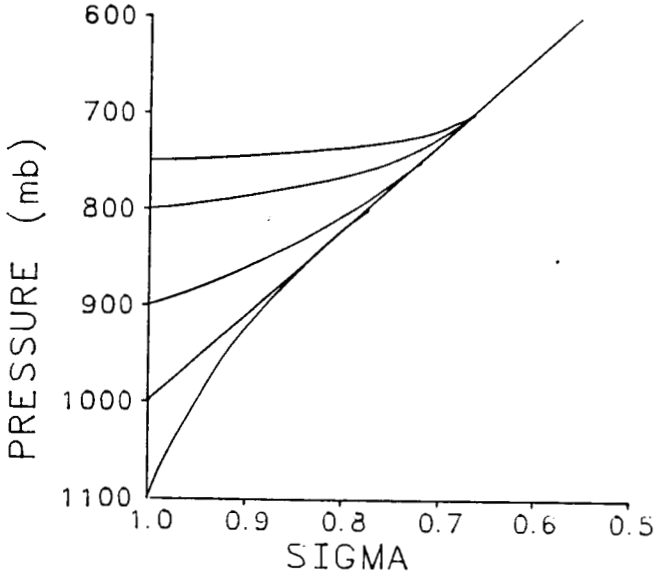

Fig 2

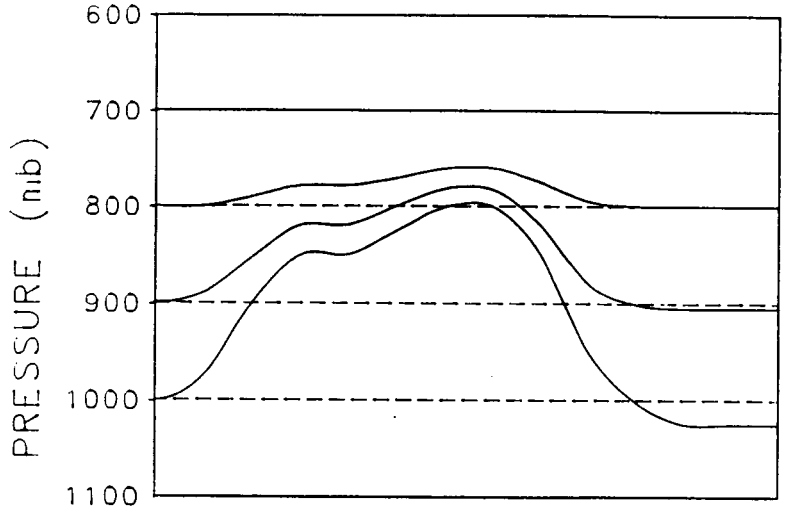

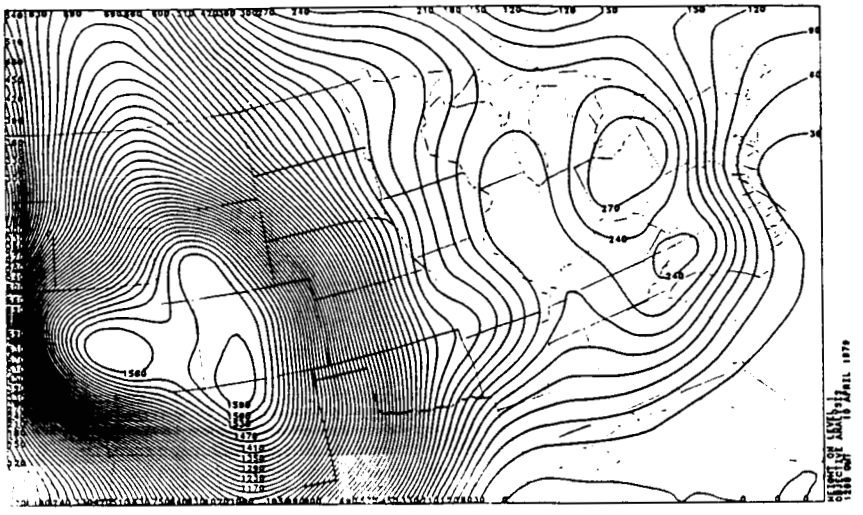

Fig. 3a

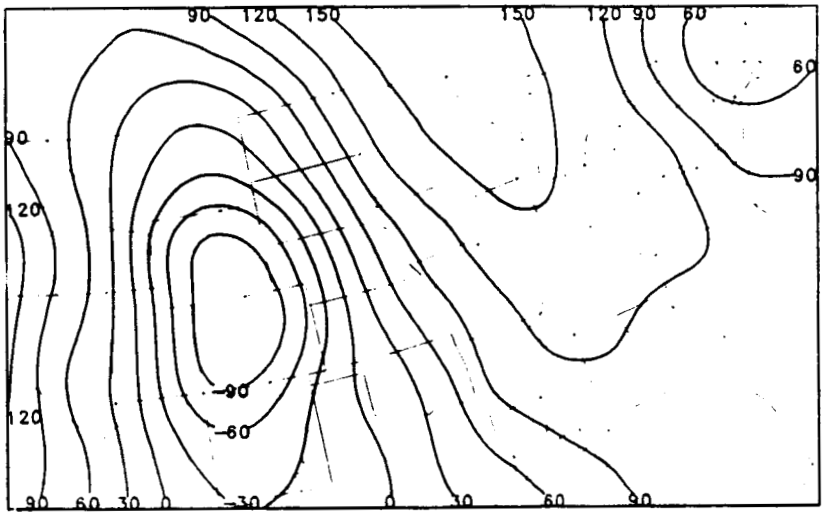


Fig. 3b

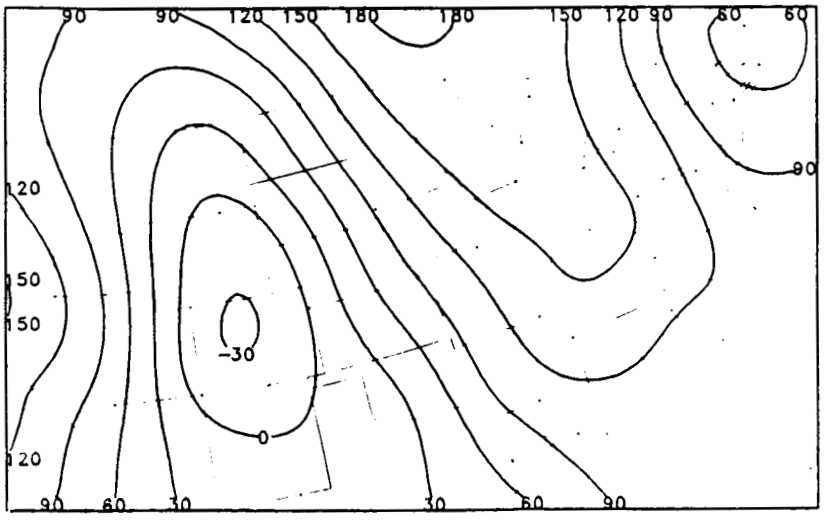


Fig.3c

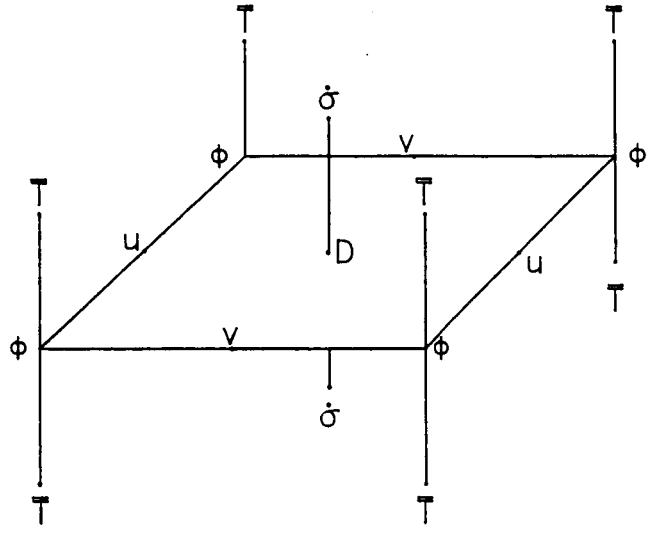


Fig 4